Available online at www.sciencedirect.com
SCIENCE DIRECT®
Journal of Sound and Vibration 265 (2003) 1063–1074
JOURNAL OF SOUND AND VIBRATION
www.elsevier.com/locate/jsvi

Modelling of a two-dimensional Coulomb friction oscillator

F. Xia*

Department of Informatics and Mathematical Modelling, Technical University of Denmark, Building 321, DK-2800, Lyngby, Denmark

Received 8 April 2002; accepted 16 July 2002

Abstract

Xia proposes a model for investigating the stick–slip motion caused by dry friction of a two-dimensional oscillator under arbitrary excitations. Instead of the harmonic balance method used by most investigators, a numerical approach to investigate the system is provided. The concept of the *friction direction angle* is introduced to determine the components of the static and kinetic friction force vector and the hyperbolic secant function is introduced to deal with the transition of the friction force from the static to the kinetic state. The *friction direction angle* is determined by either relative velocities or input forces. With this method the switch conditions for stick state, slip state and stick–slip state can be easily derived. The orbits of the responses, which are either straight line segments, circular or elliptic are obtained. In the general case, the orbit of the response is a complex planar curve. Zero-stop, one-stop, two-stops and more than two-stops per cycle are also found.

1. Introduction

In order to simulate the motion of a friction oscillator with a two-dimensional dry friction constraint, there are two unavoidable matters must be dealt with. One is the hysteresis induced by the dry friction coefficients of static and kinetic friction and the other is the discontinuity induced by the stick–slip motion. It is not difficult to determine the components of the kinetic friction force vector and the state friction force vector individually, but no widely accepted way to treat the stick–slip motion exists, especially not for complicated mechanical systems. Meng and Chidamparam [1] use a massless friction damper with two linear springs of finite stiffness to obtain the components of the friction force vector. However, when the stick–slip motion takes

*Tel.: +45-45-25-30-79; fax: 45-45-93-23-73.
E-mail address: xf@imm.dtu.dk (F. Xia).

0022-460X/03/$ - see front matter © 2002 Elsevier Science Ltd. All rights reserved.
doi:10.1016/S0022-460X(02)01444-X

place the formulation was not provided rigorously. The method provided in their paper is not convenient for handling the two-dimensional dry friction in complicated mechanical systems.

For some special cases, the excitations are sinusoidal with the same frequency and with different amplitudes or phases and the orbits of responses will be reduced to straight line segments or to circular or elliptic shapes. In these cases the harmonic-balance method is widely used to give an analytical approximate solution [1–5]. However, for complicated excitations, e.g., sinusoidal excitations with different frequencies in two orthogonal directions or even time series, the orbit of the response will become a complex self-intersecting planar curve, and in this case the harmonic-balance method fails.

For dynamic systems with dry friction, Den Hartog [6] presented a closed-form solution as early as in 1931 for the steady-state zero-stop response of a harmonically excited oscillator with Coulomb friction. Since then one-stop, two- and multiple-stops per cycle have been reported [7]. Responses with bifurcations and chaos have also been found in many fields [8–11], but most of the research efforts have focused on one-dimensional dry friction models, which means that the motion is along a straight line.

The two-dimensional Coulomb friction oscillator has wide applications in the fields of the freight-bogies on railways, turbo-machinery, earth quake theory and robot-walking mechanisms. Here our attention mainly shall be turned towards applications to the so-called wedge dampers in the three-piece-freight-bogie and dry friction dampers in the bogie Y25. In both cases they are used to dissipate the vibration energy produced by the interaction between wheels and rails [12–14]. Up to now, only a few reports on the response of wedge dampers with two-dimensional dry friction have been published. In order to understand the dynamical performances of the wedge damper, which basically is a two-dimensional dry friction oscillator, the responses of a two-dimensional dry friction oscillator should first be understood and implement a basic numerical method. For the non-linear discontinuous dynamic systems with complex excitations in orthogonal directions, an analytical solution cannot be found, so numerical methods must be used.

In Section 2 a mass–spring system with the mass sliding along a dry surface when it is subjected to an external force is modelled. The friction direction angle and the determination of the components of the friction force vector are discussed in Section 3. The stick–slip motion analysis is discussed in Section 4; and the numerical simulation, some results and discussions of the system are provided in Section 5.

2. Description of a two-dimensional friction oscillator

Consider the two-dimensional friction oscillator shown in Fig. 1. The mass m is in contact with a plane surface and it is connected to fixed walls by two linear springs and two linear viscous dampers along the x and y directions, respectively. Newton's second law applies, and the equations of motion of the system can easily be written as

$$m\ddot{x} + c_x\dot{x} + k_x x + F_{x\mu} = F_x, \tag{1}$$

$$m\ddot{y} + c_y\dot{y} + k_y y + F_{y\mu} = F_y, \tag{2}$$

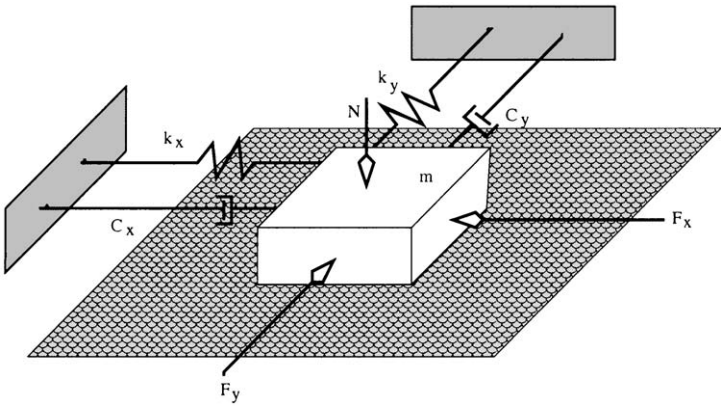

Fig. 1. A two-dimensional friction oscillator.

where the components of the friction forces $F_{x\mu}$ and $F_{y\mu}$ must satisfy the relation:

$$F_\mu = \sqrt{F_{x\mu}^2 + F_{y\mu}^2} \leqslant \mu N, \tag{3}$$

where N is the normal force on the mass, which in general is a state-dependent variable, for the sake of simplicity it is assumed to be constant. μ is the friction coefficient, which has two states: a static coefficient of friction μ_s, and a kinetic coefficient of friction μ_k. The friction force can therefore be written as $F_\mu = -Nf(V)$, where $f(V)$ is determined by the relation [9]

$$f(V) = \begin{cases} \mu_k & \text{if } V > 0, \\ -\mu_s \leqslant f(V) \leqslant \mu_s & \text{if } V = 0, \\ -\mu_k & \text{if } V < 0. \end{cases} \tag{4}$$

The velocity V of the mass has the components $\dot{x}$ and $\dot{y}$, which determine the direction of the kinematic friction force. It reads

$$|V| = \sqrt{\dot{y}^2 + \dot{x}^2}. \tag{5}$$

The derivatives of x and y are with respect to the time τ. The friction direction angle between $\dot{x}$ and $\dot{y}$ is defined by

$$\theta = \begin{cases} \tan^{-1}(\dot{y}/\dot{x}), & (\dot{x} \geqslant 0,\ \dot{y} \neq 0), \\ \pi - \tan^{-1}(\dot{y}/\dot{x}), & (\dot{x} < 0,\ \dot{y} \geqslant 0), \\ \pi + \tan^{-1}(\dot{y}/\dot{x}), & (\dot{x} < 0,\ \dot{y} < 0). \end{cases} \tag{6}$$

Hence, the components of the friction forces can be expressed in the following way:

$$F_{x\mu} = F_\mu \cos\theta, \quad F_{y\mu} = F_\mu \sin\theta. \tag{7}$$

The driving forces F_x and F_y are arbitrary but in the present paper they are assumed to be simple harmonic functions with driving (angular) frequencies ω_{xd} and ω_{yd}, respectively:

$$F_x = f_{x0} \cos(\omega_{xd}\tau + \phi_x), \quad F_y = f_{y0} \cos(\omega_{yd}\tau + \phi_y), \tag{8}$$

where f_{x0} and f_{y0} are the amplitudes and ϕ_x and ϕ_y are the phases.

In the case of $k_x = k_y = k$ and $c_x = c_y = c$, the time and the displacements may be rescaled as

$$x_s = \frac{kx}{N}, \quad y_s = \frac{ky}{N}, \quad t = \tau\sqrt{k/m}, \quad \omega_{xd} = \Omega_x\sqrt{m/k}, \quad \omega_{yd} = \Omega_y\sqrt{m/k}. \tag{9}$$

Eqs. (1) and (2) can then be written in dimensionless form:

$$\ddot{x}_s + \xi\dot{x}_s + x_s + f(\mu)\cos\theta = \beta_x\cos(\Omega_x t + \phi_x), \tag{10}$$

$$\ddot{y}_s + \xi\dot{y}_s + y_s + f(\mu)\sin\theta = \beta_y\cos(\Omega_y t + \phi_y), \tag{11}$$

where

$$\beta_x = f_{x0}/N, \quad \beta_y = f_{y0}/N, \quad \xi = c/\sqrt{km} \tag{12}$$

and the friction direction angle θ remains in the same form as Eq. (6) except that $\dot{x}$ and $\dot{y}$ are replaced by $\dot{x}_s$ and $\dot{y}_s$.

3. The friction direction angle and the components of the friction force vector

In order to define a friction force vector on a plane, its modulus and argument must be known. The modulus of the friction force vector is determined by Eqs. (3) and (4), and its argument is given by the angle θ shown in Fig. 2. Then the x and y components of the friction force can be determined. The angle θ is called the *friction direction angle*. The dry friction is assumed to be isotropic.

If the velocity components $V_x = \dot{x}$ and $V_y = \dot{y}$ of the mass are different from $(0, 0)$ then the friction direction angle is determined by the angle between the velocity V_x and the resultant velocity V. The modulus of the friction force vector is then equal to the normal force times the kinetic friction coefficient, viz. $F_\mu = N_{\mu k}$. The direction of the friction force is opposite to the resultant velocity V as shown in Fig. 2(a) due to the isotropy. The friction direction angle is given by the velocities V_x and V_y in Eq. (6), and then the components of the friction force vector are given by Eq. (7).

If (V_x, V_y) equals $(0, 0)$ then the maximum value of the friction force is equal to the normal force times the static friction coefficient, viz. $F_\mu = N_{\mu s}$, and the corresponding components of the friction force are equal to the corresponding input forces, viz. $F_{x\mu} = F_{inx}$, $F_{y\mu} = F_{iny}$. Although

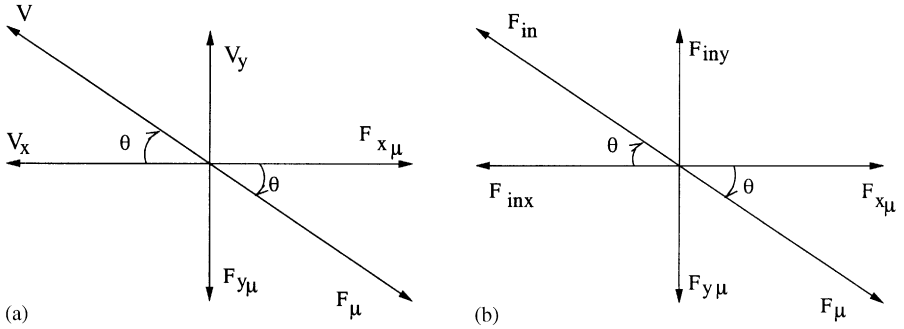

Fig. 2. The friction direction angle in a two-dimensional friction oscillator.

the mass is in rest, the friction force is not zero. This state is called a *non-zero static friction force equilibrium state*, and the friction force vector is equal and opposite to the input force, which is shown in Fig. 2(b). The effect of the torque caused by the input force and friction force is neglected in the present paper. In other words, the input forces F_{inx} and F_{iny} can be used to determine the friction direction angle alternatively, viz.

$$\theta = \begin{cases} \tan^{-1}(F_{iny}/F_{inx}) & (F_{inx} \geqslant 0,\ F_{iny} \neq 0), \\ \pi - \tan^{-1}(F_{iny}/F_{inx}) & (F_{inx} < 0,\ F_{iny} \geqslant 0), \\ \pi + \tan^{-1}(F_{iny}/F_{inx}) & (F_{inx} < 0,\ F_{iny} < 0). \end{cases} \tag{13}$$

When both the velocities and the input forces of the mass are equal to zero, then the friction force is zero and the system is also in equilibrium. This state is called a *zero friction force equilibrium state*. In this case the friction direction angle is undetermined.

The definition of the friction direction angle, θ is now extended to include the two cases in Eqs. (6) and (13). It is determined in the following way:

$$\theta = \begin{cases} \chi(\dot{x}_s, \dot{y}_s) & (\dot{x}_s \vee \dot{y}_s \neq 0), \\ \psi(F_{inx}, F_{iny}) & (\dot{x}_s \wedge \dot{y}_s = 0,\ F_{inx} \vee F_{iny} \neq 0), \\ \emptyset & (\dot{x}_s \wedge \dot{y}_s \wedge F_{inx} \wedge F_{iny} = 0), \end{cases} \tag{14}$$

where $\chi(\dot{x}_s, \dot{y}_s)$ denotes the representation of θ by (6); $\psi(F_{inx}, F_{iny})$ stands for the representation of θ by Eq. (13) and $\emptyset$ is the empty set of θ. The symbol $\vee$ means disjunction and the $\wedge$ denotes conjunction. As a consequence, the components of the friction force vector in the two orthogonal directions can be determined by the following formulae:

$$\left.\begin{aligned} F_{x\mu k} &= F_\mu \cos\theta \\ F_{y\mu k} &= F_\mu \sin\theta \end{aligned}\right\} \quad \begin{aligned} &(\dot{x}_s \wedge \dot{y}_s \neq 0) \mid (\dot{x}_s \wedge \dot{y}_s = 0, \\ &|F_{inx}| \geqslant |F_{x\mu s}|, |F_{iny}| \geqslant |F_{y\mu s}|), \end{aligned} \tag{15}$$

$$\left.\begin{aligned} F_{x\mu t} &= F_{inx} \\ F_{y\mu t} &= F_{iny} \end{aligned}\right\} \quad (\dot{x}_s \wedge \dot{y}_s = 0, |F_{inx}| < |F_{x\mu s}|, |F_{iny}| < |F_{y\mu s}|). \tag{16}$$

Note that the components of the maximum friction force vector in the x and y directions, $F_{x\mu s}, F_{y\mu s}$ that are used in the conditions are determined by

$$\begin{aligned} F_{x\mu s} &= \Re(\theta) N \mu_s \cos\theta, \\ F_{y\mu s} &= \Re(\theta) N \mu_s \sin\theta. \end{aligned} \tag{17}$$

where the function $\Re(\theta)$ is defined as

$$\Re(\theta) = \begin{cases} 1, & \theta \in \Theta, \\ 0, & \theta \notin \Theta \end{cases} \tag{18}$$

in which the symbol Θ stands for a non-empty set of θ. Eq. (18) is used to determined the stick–slip switch conditions as it can be seen in the next section.

In the case of a one-dimensional friction oscillator, the friction direction angle reduces to 0 or π (motion in x direction) or $\pi/2$ or $3\pi/2$ (motion in y direction). Therefore, the friction direction angle can be used to instead of the sign function.

4. Stick–slip motion analysis

4.1. The resultant force and input force

When the resultant velocity of the mass is equal to zero, it is said that the system is in the stick-phase. In this case the friction coefficient attains its maximum value μ_s and the associated friction force may reach its maximum value, which is the same as the definition of the maximum static friction force. If the acting force (input force) is less than the static friction force there is no motion occurring, because the static friction force will balance the input force. If the input force is larger than the static friction force, the balance will break and the mass will move under the action of the input force and the friction force with the kinetic friction coefficient μ_k. The resulting motion is a consequence of the stick–slip action of the friction force. In order to deal with the stick–slip motion, the friction direction angle and the determination of the related components of the friction force vector can be used, which have just been discussed in the previous section.

In the case of a moving mass, which is called the slip-phase, the resultant forces are

$$F_{xh} = F_{inx} - F_{x\mu k}, \tag{19}$$

$$F_{yh} = F_{iny} - F_{y\mu k} \tag{20}$$

and if the mass comes to rest, which is called the stick-phase, the resultant forces are

$$F_{xl} = F_{inx} - F_{x\mu}, \tag{21}$$

$$F_{yl} = F_{iny} - F_{y\mu}, \tag{22}$$

where $F_{x\mu}, F_{y\mu}$ denote the acting friction forces. They are equal to $F_{x\mu k}, F_{y\mu k}$ for the slip-phase and $F_{x\mu t}, F_{y\mu t}$ for the stick-phase, respectively. The friction forces $F_{x\mu k}, F_{y\mu k}, F_{x\mu t}, F_{y\mu t}$ are determined by Eqs. (15) and (16). The input forces are defined by

$$F_{inx} = \beta_x \cos(\Omega_x t + \phi_x) - \xi \dot{x}_s - x_s, \quad F_{iny} = \beta_y \cos(\Omega_y t + \phi_y) - \xi \dot{y}_s - y_s, \tag{23}$$

which may be used to find the friction direction angle.

The dependence of the friction coefficient on the relative velocity, was determined in three ways in Ref. [10]. Here a fourth approximate description is used [15,16].

In order to obtain a continuous transition of the friction forces from zero to non-zero speeds as a weight function the hyperbolic secant function is introduced

$$\operatorname{sech}(\eta) = \frac{2}{(e^{-\eta} + e^{\eta})}. \tag{24}$$

To this end, the resulting forces acting on the mass at arbitrary speeds are defined as

$$F_{rx} = F_{xl} \operatorname{sech}(\dot{x}_s \alpha) + F_{xh}(1 - \operatorname{sech}(\dot{x}_s \alpha)), \tag{25}$$

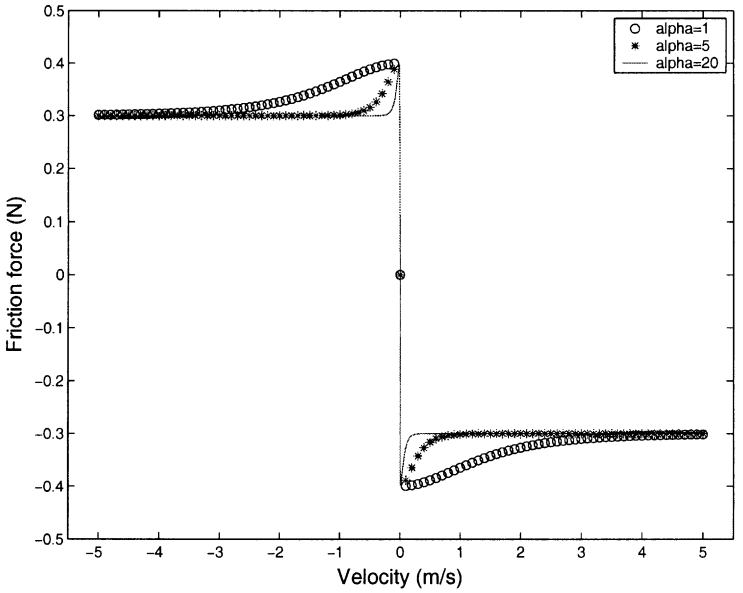

Fig. 3. The friction force with unit normal force as a function of the velocity for different parameter values α.

$$F_{ry} = F_{yl}\,\mathrm{sech}(\dot{y}_s\alpha) + F_{yh}(1 - \mathrm{sech}(\dot{y}_s\alpha)), \tag{26}$$

where α is a parameter that is related to the speed of the mass. A specified value of α provides the corresponding approximate friction characteristics.

This model is well suited for the numerical implementation since the user remains in control of the numerical process during the switch from stick to slip. Fig. 3 shows the curves of friction force as a function of the speed for various values of the parameter α.

Finally, the dynamical equation reads:

$$\begin{bmatrix} m & 0 \\ 0 & m \end{bmatrix} \begin{bmatrix} \ddot{x}_s \\ \ddot{y}_s \end{bmatrix} = \begin{bmatrix} F_{rx} \\ F_{ry} \end{bmatrix}. \tag{27}$$

4.2. Conditions for stick–slip motions

If the input forces satisfy the condition

$$|F_{inx}| > |F_{x\mu s}| \vee |F_{iny}| > |F_{y\mu s}| \tag{28}$$

or

$$\sqrt{F_{inx}^2 + F_{iny}^2} > |F_{\mu}| \tag{29}$$

then the mass will change from the stick phase, to the slip phase.

When the system is in the slip phase, if it change to the stick phase the input forces must satisfy the following conditions:

$$|F_{inx}| < |N\mu_s \cos\theta \,\mathrm{sech}(\alpha\dot{x}_s) + N\mu_k \cos\theta(1 - \mathrm{sech}(\alpha\dot{x}_s))|,$$
$$|F_{iny}| < |N\mu_s \sin\theta \,\mathrm{sech}(\alpha\dot{y}_s) + N\mu_k \sin\theta(1 - \mathrm{sech}(\alpha\dot{y}_s))|. \quad (30)$$

During the slip-phase changing to stick-phase the velocity will change continuously. When the motion into the stick phase the components of the friction force vector are determined by Eq. (16).

5. Characteristics of the two-dimensional friction oscillator

5.1. Special cases of the system

If the external force in Eqs. (10) and (11) along the y(or x) direction is zero, it means that the mass only moves along the x(or y) direction. In this case the problem reduces to a one-dimensional friction oscillator, which has been investigated by many researchers [1,6–10]. With the method introduced above, the friction direction angel θ then is either 0 or π, so the sign function can be replaced by the friction direction angle.

If two excitation forces share the relations $\Omega_x = \Omega_y$ and $\phi_x = \phi_y$, then

$$\frac{\beta_x \cos(\Omega_x t + \phi_x)}{\beta_y \cos(\Omega_y t + \phi_y)} = Constant. \quad (31)$$

Then there is a linear relation between the two friction force components, and Eqs. (10) and (11) can be reduced to a one-dimensional dynamic system:

$$\ddot{z} + c\dot{z} + z + \mu\theta_0 = \beta_z \cos(\Omega_z t + \phi), \quad (32)$$

where the θ_0 takes the values of 0 or π and the orbit of the response is a straight line segment.

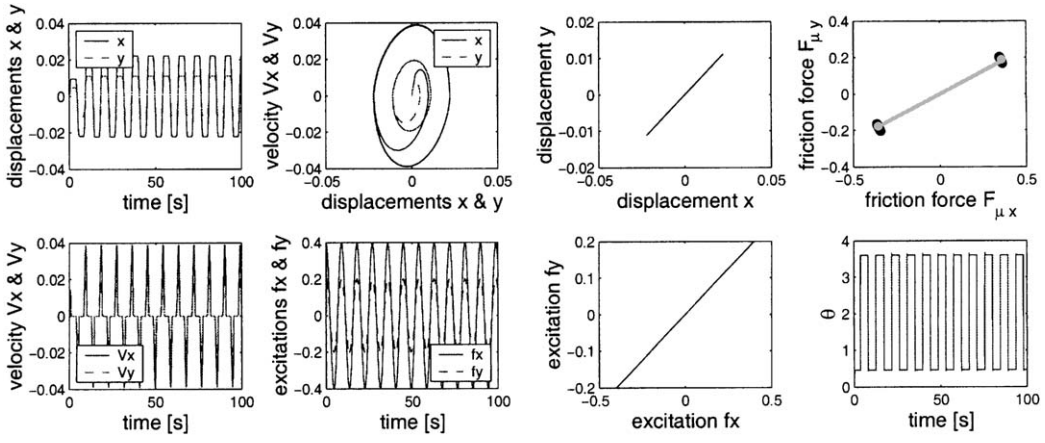

Fig. 4. The straight line segment orbit of the response to different amplitudes and the same frequencies of excitations. Left fours: responses and phase diagrams; Right fours: friction forces and friction direction angles.

In order to show this, the parameter values are chosen as: $\mu_s = \mu_k = 0.4,\ \beta_x = 0.4,\ \beta_y = 0.2$ and $\Omega_x = \Omega_y = 0.7,\ \xi_x = \xi_y = 0.5,\ \phi_x = \phi_y = 0$. The simulation results are shown in Fig. 4, in which the four left plots show the displacements and the phase diagram; and the right four plots show the friction force (in the figure the limit friction force overlaps the acting friction force) and the friction direction angle.

For $c_x = c_y,\ k_x = k_y$, i.e., a symmetric system, the response will have a circular orbit when the mass is excited by a sinusoidal excitation where the x and y components differ in phase by $\pi/2$ [1]. The results are shown in Fig. 5 for comparison with the results in Ref. [1]. In the figure, the left four plots show the displacements, the phase diagram, the velocities and the exciting forces. If the amplitudes of the exciting forces are large enough then the acting friction force is identical to the limiting locus of the friction force. In the case where the amplitudes of the exciting forces are small as shown in the right four plots of Fig. 5, then the acting friction force is less than the limiting locus of the friction force and obviously the system is in rest. In the figure, the dotted circle denotes the limiting locus of the friction force and the solid circle shows the acting friction force.

The orbit of the response will be elliptic under the excitations

$$\Omega_x = \Omega_y, \quad \phi_x \neq \phi_y \tag{33}$$

and the difference in phase differs from $\pi/2$. Letting the parameters $\beta_x = \beta_y = 0.5,\ \Omega_x = \Omega_y = 0.2,\ k_x = k_y = 1,\ \xi_x = \xi_y = 1,\ \phi_x = 0, \phi_y = \pi/4$ and $\mu_k = \mu_s = 0.4$. The displacements, the phase diagram, the orbit of the response, the friction forces and the friction direction angles are shown in Fig. 6. It is easy to see that there exist two stops per cycle. Correspondingly, in the plot of the acting friction force $F_{\mu y}$ versus $F_{\mu x}$ the circle is seen to be divided into two segments with a gap around $F_{\mu y} = 0$. Therefore the acting friction force is inside or on the limiting locus of the friction force. This means that there are two stick states per cycle. When the static coefficient of friction equals the kinematic coefficient of friction, the curve of the limiting locus of the friction force on the two-dimensional plane is a circle.

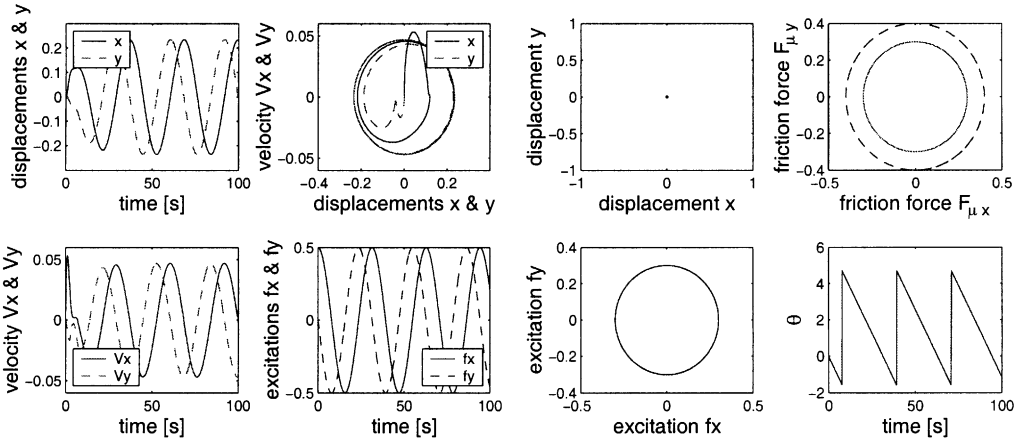

Fig. 5. Left: responses to sinusoidal excitations differing in phase by $\pi/2$; $\mu_s = \mu_k = 0.4\ \beta_x = \beta_y = 0.5,\ k_x = k_y = 1,\ \xi_x = \xi_y = 1,\ \phi_x = 0,\ \phi_y = \pi/2$. Right: the trajectory, the friction forces and the friction direction angle with the parameters are same as the left except $\beta_x = \beta_y = 0.3$.

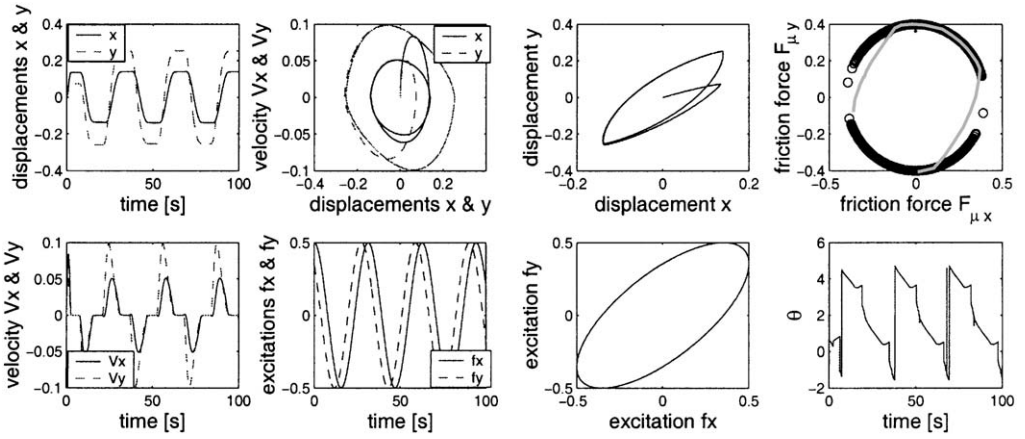

Fig. 6. Responses of the stick–slip state in which the orbit is elliptic: $\mu_s = \mu_k = 0.4,\ \beta_x = \beta_y = 0.5,\ \Omega_x = \Omega_y = 0.2,\ k_x = k_y = 1,\ \xi_x = \xi_y = 1,\ \phi_x = 0, \phi_y = \pi/4$.

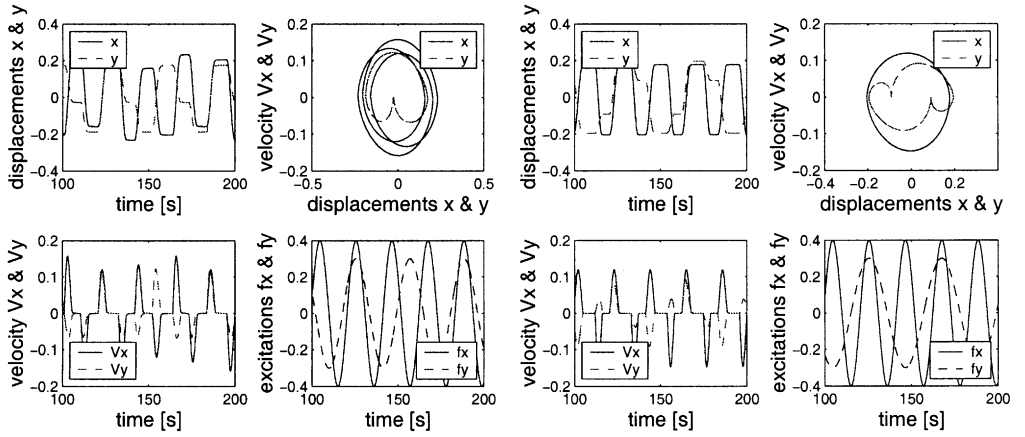

Fig. 7. Left: two and three-stops per cycle: $\mu_s = \mu_k = 0.4,\ \beta_x = 0.4,\ \beta_y = 0.3,\ \Omega_x = 0.3$ and $\Omega_y = 0.2,\ \xi_x = \xi_y = 0.5$; Right: two and four-stops per cycle along x and y directions, respectively: the parameters are same as the left except for the $\Omega_y = 0.15$.

5.2. *Multiple stops per cycle*

In the case of one-dimensional friction, there are many types of steady state behaviour: permanent sticking, zero stop per cycle (i.e., non-sticking oscillation), one-stop, two-, four-, six-stops per cycle, and so on [7]. As an example, only two- and four-stops per cycle are shown here. However, the three-stops per cycle are also found for the two-dimensional friction case. The results are shown in Fig. 7.

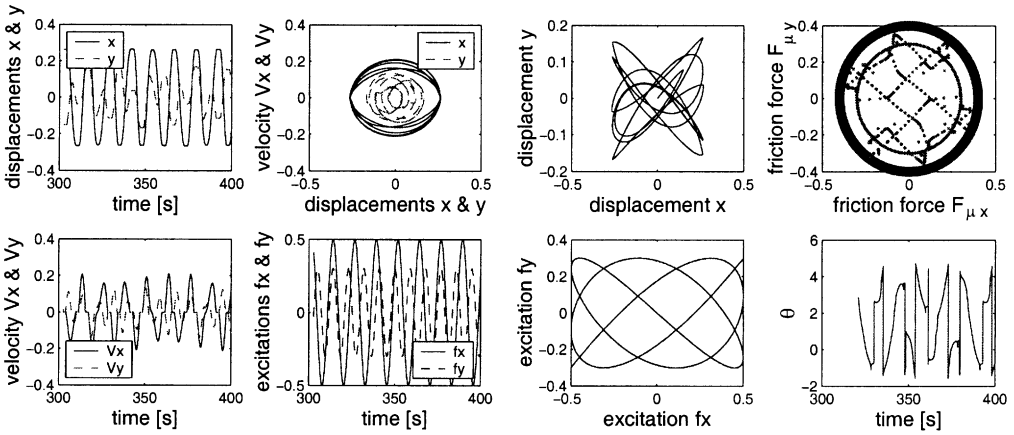

Fig. 8. Response to sinusoidal excitations with different amplitudes and frequencies: $\mu_s = 0.4$, $\mu_k = 0.3$, $\xi_x = \xi_y = 1$, $\beta_x = 0.5$, $\beta_y = 0.3$, $\Omega_x = 0.5$, $\Omega_y = 0.7$; Left fours: responses and phase diagrams; Right fours: the orbit of the response and the friction direction angle.

5.3. General responses of the system

In general case, the orbit of the response to arbitrary amplitudes and frequencies both in x and y directions is a plane curve. As an example, let the initial phases be zero. Fig. 8 shows the steady state of the displacements and the phase diagram in the left four plots of the figure. The orbit of the response and the corresponding friction direction angle are shown in the right four plots of the figure. The figure clearly shows that the orbit of the response is not a simple circle or an ellipse but a rather complex planar curve.

6. Conclusions

A method is provided to simulate the stick–slip motion of a two-dimensional dry friction oscillator under complex excitations. The friction direction angle has been defined and successfully used to replace the sign function that is widely used in the one-dimensional friction oscillator. With the friction direction angle both the module and the argument of the friction force vector can be determined for the stick state as well as for the slip state. By the switch-condition the stick–slip motion can be simulated numerically under various excitations.

The two-dimensional coupled oscillator can be uncoupled under certain conditions. The orbit of the responses of a two-dimensional friction oscillator will be a straight line segment, a circle or an ellipse depending on the details of the sinusoidal excitations. In the general case, the response is a complex planar curve. For various levels of excitations, the zero-stop, one-stop, two-stops and multiple stops per cycle will appear.

There are still some topics such as velocity-dependent friction coefficient, the collapse of the state space of the system caused by stick–slip motion and a variable normal force that need investigation. Especially, if the normal force is a state-dependent variable, the problem will

become more complicated. That case will be discussed in connection with our investigation of the model of wedge dampers in three-piece-freight-bogie on railways [16].

Acknowledgements

The work was performed under the supervision of Professor Hans True and the financial support of DSB (Danish State Railways), the Danish Research Agency and the Technical University of Denmark. I am grateful to Professor Hans True for his inspiring ideas through this work and to Professor Per Grove Thomsen for his help with numerical methods.

References

[1] C.-H. Meng, P. Chidamparam, Friction damping of two-dimensional motion and its application in vibration control, Journal of Sound and Vibration 144 (1991) 427–447.
[2] K.Y. Sanliturk, D.J. Ewins, Modelling two-dimensional friction contact and its application using harmonic balance method, Journal of Sound and Vibration 193 (1996) 511–523.
[3] B.D. Yang, M.L. Chu, C.H. Meng, Stick–slip-separation analysis and non-linear stiffness and damping characterization of friction contacts having variable normal load, Journal of Sound and Vibration 201 (1998) 461–481.
[4] B.D. Yang, C.H. Meng, Characterization of 3D contact kinematics and prediction of resonant and response of structures having 3D frictional constraint, Journal of Sound and Vibration 217 (1998) 909–925.
[5] B.D. Yang, C.H. Meng, Periodic response of structures having three-dimensional frictional constraints, Journal of Sound and Vibration 229 (2000) 775–792.
[6] J.P. Den Hartog, Forced vibration with combined Coulomb and viscous friction, Transcations of the American Society of Mechanical Engineers 53 (1931) 107–115.
[7] H.-K. Hong, C.-S. Liu, Coulomb friction oscillator: modelling and responses to harmonic loads and base excitations, Journal of Sound and Vibration 229 (2000) 1171–1192.
[8] S.W. Saw, On the dynamic response of a system with dry friction, Journal of Sound and Vibration 108 (1986) 305–325.
[9] B. Feeny, A nonsmooth Coulomb friction oscillator, Physica D 59 (1992) 25–38.
[10] K. Popp et al., Series on stability, vibration and control of systems, series B: dynamics with friction: modelling, analysis and experiment, in: A. Guran, F. Pfeiffer, K. Popp (Eds.), Analysis of a Self Excited Friction Oscillator with External Excitation, Vol. 7, pp. 1–35.
[11] H. True, On the theory of non-linear dynamics and its applications in vehicle systems dynamics, Vehicle System Dynamics 31 (1999) 393–421.
[12] J.F. Gardner, J.P. Cusumano, Dynamic models of friction wedge dampers, Proceedings of the ASME/IEEE Joint Railroad Conference, Boston, MA, 1997, pp. 65–69.
[13] R.D. Fröhling, The influence of friction wedges on the dynamic performance of three-piece self bogies, Proceedings of the Fourth International Conference on Railway Bogies and Gears, Budapest, 1998, pp. 95–103.
[14] J.R. Evans, P.J. Rogers, Validation of dynamic simulations of rail vehicles with friction damped Y25 bogies, Vehicle System Dynamics Supplement 28 (1998) 219–233.
[15] H. True, R. Asmund, The dynamics of a railway freight wagon wheelset with dry friction damping, Vehicle System Dynamics 38 (2002) 149–163.
[16] F. Xia, Modelling of wedge dampers in the presence of two-dimensional dry friction, Proceedings of the 17th IAVSD Symposium, Copenhagen, Denmark, August 20–24, 2001.